



A generalized-Laguerre–Hermite pseudospectral method for computing symmetric and central vortex states in Bose–Einstein condensates

Weizhu Bao^{a,*}, Jie Shen^b

^aDepartment of Mathematics and Center for Computational Science and Engineering, National University of Singapore, Singapore 117543, Singapore

^bDepartment of Mathematics, Purdue University, West Lafayette, IN 47907, USA

ARTICLE INFO

Article history:

Received 8 March 2008

Received in revised form 4 July 2008

Accepted 24 July 2008

Available online 11 August 2008

Keywords:

Generalized-Laguerre–Hermite functions

Bose–Einstein condensate

Central vortex state

Symmetric state

Normalized gradient flow

ABSTRACT

A generalized-Laguerre–Hermite pseudospectral method is proposed for computing symmetric and central vortex states in Bose–Einstein condensates (BECs) in three dimensions with cylindrical symmetry. The new method is based on the properly scaled generalized-Laguerre–Hermite functions and a normalized gradient flow. It enjoys three important advantages: (i) it reduces a three-dimensional (3D) problem with cylindrical symmetry into an effective two-dimensional (2D) problem; (ii) it solves the problem in the whole space instead of in a truncated artificial computational domain and (iii) it is spectrally accurate. Extensive numerical results for computing symmetric and central vortex states in BECs are presented for one-dimensional (1D) BEC, 2D BEC with radial symmetry and 3D BEC with cylindrical symmetry.

© 2008 Elsevier Inc. All rights reserved.

1. Introduction

Quantized vortices play an important role in verifying the superfluid properties of quantum fluids such as Bose–Einstein condensates (BECs) or degenerate Fermi gases. In weakly interacting alkali gases, condensate states containing a single vortex line were first created using Raman transition phase-imprinting method [22]. Later, multiply charged vortices were created by using topological phase engineering methods [18]. It is expected that more complicated vortex clusters can be created in the future, e.g. with the further development of the phase-imprinting method. Such states would enable various opportunities, ranging from investigating the properties of random polynomials [9] to using vortices in quantum memories [15]. All of these experimental developments stir a great interest in the study of states with several vortices. Recently, there were a number of investigations on the properties of quantized vortices in BECs, e.g. dynamical stability and interaction laws between a few vortices [25,17,14,21]. To study these problems effectively, a key issue is to find efficiently and accurately central vortex states in BECs.

In this paper, we consider a Bose–Einstein condensate (BEC) in a cylindrically symmetric trap $V_t(x, y, z) = \frac{1}{2}m_b(\omega_r^2(x^2 + y^2) + \omega_z^2z^2) + W_t(z) = \frac{1}{2}m_b(\omega_r^2r^2 + \omega_z^2z^2) + W_t(z)$ with $r = \sqrt{x^2 + y^2}$, ω_r and ω_z the trap frequencies in radial and axial direction, respectively, m_b the mass of BEC atoms, and $W_t(z)$ is a real-valued bounded function of z . We assume that the interaction strength within the BEC is U_0 , given by $U_0 = 4\pi\hbar^2a_s/m_b$ with a_s the s-wave scattering length. For temperatures well below the critical temperature of the BEC, the dynamics of the BEC is well described by the dimensionless 3D Gross–Pitaevskii equation (GPE) [24]

* Corresponding author. Fax: +65 67746756.

E-mail addresses: bao@math.nus.edu.sg (W. Bao), shen@math.purdue.edu (J. Shen).

URL: <http://www.math.nus.edu.sg/~bao/> (W. Bao).

$$i \frac{\partial}{\partial t} \psi = \left[-\frac{1}{2} \left(\frac{\partial^2}{\partial x^2} + \frac{\partial^2}{\partial y^2} + \frac{\partial^2}{\partial z^2} \right) + \frac{1}{2} (\gamma_r^2 r^2 + \gamma_z^2 z^2) + W(z) + \beta |\psi|^2 \right] \psi. \quad (1.1)$$

Here, $\psi = \psi(x, y, z, t)$ is the normalized wave function of the condensate with

$$\|\psi(x, y, z, t)\|^2 = \int_{\mathbb{R}^3} |\psi(x, y, z, t)|^2 dx dy dz = 1, \quad (1.2)$$

$\gamma_r = \frac{\omega_r}{\omega}$, $\gamma_z = \frac{\omega_z}{\omega}$ with $\omega = \min\{\omega_r, \omega_z\}$; $\beta = \frac{4\pi N a_s}{a_0}$ characterizes the inter-atomic interaction in terms of the total number of particles N in the condensate and the s-wave scattering length a_s . $W(z)$ is a dimensionless real-valued bounded function. The above dimensionless quantities in three dimensions (3D) are obtained by scaling the length by the harmonic oscillator length $a_0 = \sqrt{\hbar/m_b \omega}$, the time by ω^{-1} and the energy by $\hbar\omega$.

To find cylindrical symmetric states ($m = 0$) and central vortex line states with index or winding number m ($m \neq 0$) for the BEC, we write

$$\psi(x, y, z, t) = e^{-i\mu_m t} \phi_m(x, y, z) = e^{-i\mu_m t} \phi_m(r, z) e^{im\theta}, \quad (1.3)$$

where (r, θ, z) is the cylindrical coordinates, μ_m is the so called chemical potential, $\phi_m = \phi_m(r, z)$ is a function independent of time t and angle θ . Denoting

$$B_m^r \phi := \frac{1}{2} \left[-\frac{1}{r} \frac{\partial}{\partial r} \left(r \frac{\partial}{\partial r} \right) + \gamma_r^2 r^2 + \frac{m^2}{r^2} \right] \phi, \quad B^z \phi := \frac{1}{2} \left[-\frac{\partial^2}{\partial z^2} + \gamma_z^2 z^2 \right] \phi, \quad B_m := B_m^r + B^z. \quad (1.4)$$

Plugging (1.3) into the GPE (1.1) and the normalization condition (1.2), we obtain (see [8] for more detail)

$$\mu_m \phi_m = [B_m + W(z) + \beta |\phi_m|^2] \phi_m, \quad (r, z) \in (0, +\infty) \times (-\infty, +\infty), \quad (1.5)$$

$$\phi_m(0, z) = 0 \quad (\text{for } m \neq 0), \quad -\infty < z < \infty, \quad (1.6)$$

$$\lim_{r \rightarrow \infty} \phi_m(r, z) = 0, \quad -\infty < z < \infty, \quad \lim_{|z| \rightarrow \infty} \phi_m(r, z) = 0, \quad 0 \leq r < \infty, \quad (1.7)$$

under the normalization condition

$$\|\phi_m\|^2 = 2\pi \int_0^\infty \int_{-\infty}^\infty |\phi_m(r, z)|^2 r dr dz = 1. \quad (1.8)$$

This is a nonlinear eigenvalue problem for (μ_m, ϕ_m) under the constraint (1.8).

Once the eigenfunction ϕ_m is known, the eigenvalue (or chemical potential) μ_m can be computed by

$$\mu_m = \pi \int_0^\infty \int_{-\infty}^\infty \left[|\partial_r \phi_m|^2 + |\partial_z \phi_m|^2 + \left(\gamma_r^2 r^2 + \frac{m^2}{r^2} + \gamma_z^2 z^2 + 2W(z) \right) |\phi_m|^2 + 2\beta |\phi_m|^4 \right] r dr dz := \mu(\phi_m). \quad (1.9)$$

In [3], a backward Euler finite difference (BEFD) method was used to discretize a normalized gradient flow for computing the above symmetric and central vortex line states in the BEC. In the method, the original whole space was replaced by a truncated computational domain with an artificial boundary condition (usually homogeneous Dirichlet boundary conditions are applied). The method is formally second order accurate in space. However, how to choose an appropriately truncated computational domain is a subtle problem in practice: if it is too large, the computational resource is wasted; if it is too small, the boundary effects will contaminate the accuracy and lead to wrong solutions.

A main purpose of this paper is to develop an efficient numerical method which is spectrally accurate in space and robust for all $m \geq 0$. This is achieved by discretizing the normalized gradient flow in the whole space directly using properly scaled generalized-Laguerre and Hermite functions as basis functions. These basis functions are scaled in such a way that they become eigenfunctions of the linear operator B_m . We then use a special time discretization procedure which, while preserving the normalization and energy diminishing, does not require solving any linear system by taking advantage of the eigenfunction expansion.

The paper is organized as follows: in the next section, we describe the normalized gradient flow and its time discretization. In Section 3, we construct eigenfunctions of B_m using properly scaled generalized-Laguerre and Hermite functions, and introduce the interpolation operators based on the scaled generalized-Laguerre and Hermite Gauss quadrature. We present in Section 4 pseudospectral methods based on the scaled generalized-Laguerre and Hermite functions for computing ground state in 1D BEC, symmetric and central vortex states in 2D BEC with radial symmetry and in 3D BEC with cylindrical symmetry. In Section 5, we present numerical results on symmetric and central vortex states to demonstrate the efficiency and accuracy of our new numerical methods. Finally, some concluding remarks are drawn in Section 6.

2. Normalized gradient flow and its time discretization

In this section, we describe a time discretization procedure for solving the nonlinear eigenvalue problem (1.5)–(1.7).

The nonlinear eigenvalue problem (1.5)–(1.8) can also be viewed as the Euler–Lagrangian equations of the energy functional $E(\phi_m)$, defined as

$$E(\phi_m) = \pi \int_0^\infty \int_{-\infty}^\infty \left[|\partial_r \phi_m|^2 + |\partial_z \phi_m|^2 + \left(\gamma_r^2 r^2 + \frac{m^2}{r^2} + \gamma_z^2 z^2 + 2W(z) \right) |\phi_m|^2 + \beta |\phi_m|^4 \right] r dr dz, \quad (2.1)$$

under the constraint (1.8).

From a mathematical point of view, the symmetric states ($m = 0$) and central vortex line states with index m ($m \neq 0$) of the BEC are defined as the minimizer of the following nonconvex minimization problem:

Find $\mu_m^g \in \mathbb{R}$ and $\phi_m^g \in S_m$ such that

$$\begin{aligned} E_g &:= E(\phi_m^g) = \min_{\phi \in S_m} E(\phi), \\ \mu_m^g &= \mu(\phi_m^g) = E_g + \pi \beta \int_0^\infty \int_{-\infty}^\infty |\phi_m^g(r, z)|^4 r dr dz, \end{aligned} \quad (2.2)$$

where

$$S_m = \{\phi_m = \phi_m(r, z) \mid \|\phi_m\| = 1; \phi_m(0, z) = 0 \text{ when } m \neq 0, E(\phi_m) < \infty\}.$$

When $\beta \geq 0$, it is well known that there exists a unique positive minimizer of the nonconvex minimization problem (2.2) [19,8]. It is easy to show that the minimizer ϕ_m^g is an eigenfunction of (1.5)–(1.8). In fact, the symmetric state is also the ground state of the BEC in this case [3].

Various algorithms for computing the symmetric and central vortex line states of BEC has been proposed in the literature [10,3,8,23,1]. One of the popular and efficient techniques for dealing with the normalization constraint (1.8) is through the following procedure: Choose a time step $\Delta t > 0$ and set $t_n = n\Delta t$ for $n = 0, 1, 2, \dots$. Applying the steepest decent method to the energy functional $E(\phi)$ without constraint (1.8), and then projecting the solution back to the unit sphere S_m at the end of each time interval $[t_n, t_{n+1}]$ in order to satisfy the constraint (1.8).

It is clear that the above procedure leads to the function $\phi(r, z, t)$ which is the solution of the following normalized gradient flow:

$$\frac{\partial}{\partial t} \phi(r, z, t) = -B_m \phi - [W(z) + \beta |\phi|^2] \phi, \quad t_n \leq t < t_{n+1}, \quad n \geq 0, \quad (2.3)$$

$$\phi(0, z, t) = 0 \quad (\text{for } m \neq 0), \quad z \in \mathbb{R}, \quad t \geq 0, \quad (2.4)$$

$$\lim_{r \rightarrow \infty} \phi(r, z, t) = 0, \quad z \in \mathbb{R}, \quad \lim_{|z| \rightarrow \infty} \phi(r, z, t) = 0, \quad r \in \mathbb{R}_+, \quad (2.5)$$

$$\phi(r, z, t_{n+1}) := \phi(r, z, t_{n+1}^-) = \frac{\phi(r, z, t_{n+1}^-)}{\|\phi(\cdot, t_{n+1}^-)\|}, \quad (2.6)$$

$$\phi(r, z, 0) = \phi_0(r, z), \quad \text{with } \|\phi_0(\cdot)\| = 1, \quad (2.7)$$

where $\mathbb{R} = (-\infty, \infty)$, $\mathbb{R}_+ = (0, \infty)$, $\|\phi(\cdot)\|^2 = 2\pi \int_0^\infty \int_{-\infty}^\infty |\phi(r, z)|^2 r dr dz$, and $\phi(r, z, t_n^\pm) = \lim_{t \rightarrow t_n^\pm} \phi(r, z, t)$.

When $\beta = 0$, it can be shown as in [3] that the above normalized gradient flow is energy diminishing for any time step $\Delta t > 0$ and any initial data $\phi_0(r, z)$, i.e.

$$E(\phi(\cdot, t_{n+1})) \leq E(\phi(\cdot, t_n)) \leq \dots \leq E(\phi(\cdot, t_0)) = E(\phi_0), \quad n = 0, 1, 2, \dots, \quad (2.8)$$

which shows, rigorously, that the above algorithm for computing symmetric and central vortex line states for the BEC in the linear case is convergent. When $\beta > 0$, letting $\Delta t \rightarrow 0$ in (2.3)–(2.6), we obtain the following continuous normalized gradient flow (CNGF):

$$\frac{\partial}{\partial t} \phi(r, z, t) = \left[-B_m - W(z) - \beta |\phi|^2 + \frac{\mu(\phi(\cdot, t))}{\|\phi(\cdot, t)\|^2} \right] \phi, \quad t \geq 0, \quad (r, z) \in \mathbb{R}_+ \times \mathbb{R}$$

with the boundary conditions (2.4) and (2.5). The solution of CNGF is normalization conserved and energy diminishing provided that $\beta \geq 0$ and $W(z) \geq 0$ for all $z \in \mathbb{R}$, i.e.

$$\|\phi(\cdot, t)\|^2 \equiv \|\phi_0(\cdot)\|^2 = 1, \quad \frac{d}{dt} E(\phi(\cdot, t)) = -2 \|\partial_t \phi(\cdot, t)\|^2 \leq 0, \quad t \geq 0, \quad (2.9)$$

which in turn implies

$$E(\phi(\cdot, t_2)) \leq E(\phi(\cdot, t_1)), \quad 0 \leq t_1 \leq t_2 < \infty. \quad (2.10)$$

This shows that, when time step Δt is sufficiently small, the above algorithm for computing symmetric and central vortex line states in the nonlinear case is also convergent.

For the time discretization of (2.3)–(2.7), we adopt the following backward Euler scheme with projection:

Given ϕ^0 , find $\tilde{\phi}^{n+1}$ such that

$$\frac{\tilde{\phi}^{n+1}(r, z) - \phi^n(r, z)}{\Delta t} = -B_m \tilde{\phi}^{n+1} - (W(z) + \beta |\phi^n|^2) \tilde{\phi}^{n+1}, \quad (2.11)$$

$$\phi^{n+1}(r, z) = \frac{\tilde{\phi}^{n+1}(r, z)}{\|\tilde{\phi}^{n+1}\|}. \quad (2.12)$$

For $\beta = 0$, it is shown in [3] that

$$E(\phi^{n+1}) \leq E(\phi^n), \quad n = 0, 1, 2, \dots \quad (2.13)$$

Hence, the scheme (2.11) is energy diminishing for the linear case. However, (2.11) involves non-constant coefficients so it can not be solved by a direct fast spectral solver. Therefore, we propose to solve (2.11) iteratively (for $p = 0, 1, 2, \dots$) by introducing a stabilization term with constant coefficient

$$\frac{\tilde{\phi}^{n+1,p+1}(r, z) - \phi^n(r, z)}{\Delta t} = -(B_m + \alpha_n)\tilde{\phi}^{n+1,p+1} + (\alpha_n - W(z) - \beta|\phi^n|^2)\tilde{\phi}^{n+1,p}, \quad (2.14)$$

$$\tilde{\phi}^{n+1,0} = \phi^n, \quad \tilde{\phi}^{n+1} = \lim_{p \rightarrow \infty} \tilde{\phi}^{n+1,p}, \quad \phi^{n+1} = \frac{\tilde{\phi}^{n+1}}{\|\tilde{\phi}^{n+1}\|}. \quad (2.15)$$

The stabilization factor α_n is chosen such that the convergence of the iteration is at ‘optimal’. As the analysis in [2] shows, α_n should be chosen as

$$\alpha_n = \frac{1}{2}(b_{\min}^n + b_{\max}^n) \quad (2.16)$$

with

$$b_{\min}^n = \min_{(r,z) \in \mathbb{R}_+ \times \mathbb{R}} [W(z) + \beta|\phi^n(r, z)|^2], \quad b_{\max}^n = \max_{(r,z) \in \mathbb{R}_+ \times \mathbb{R}} [W(z) + \beta|\phi^n(r, z)|^2]. \quad (2.17)$$

3. Eigenfunctions and interpolations

3.1. Eigenfunctions of B_m

As shown in the last section, the numerical scheme for (2.3)–(2.7) requires solving, repeatedly, (2.14). Therefore, it is most convenient to use eigenfunctions of B_m as basis functions. Thanks to (1.4), we only need to find eigenfunctions of B_m^r and B^z . We shall construct these eigenfunctions by properly scale the Hermite polynomials and generalized Laguerre polynomials which have been widely used in solving partial differential equations [11–13,16,20,28–30].

We start with B^z . Let $H_l(z)$ ($l = 0, 1, 2, \dots$) be the standard Hermite polynomials of degree l satisfying

$$H_l''(z) - 2zH_l'(z) + 2lH_l(z) = 0, \quad z \in \mathbb{R}, \quad l = 0, 1, 2, \dots, \quad (3.1)$$

$$\int_{-\infty}^{\infty} H_l(z)H_{l'}(z)e^{-z^2}dz = \sqrt{\pi}2^l l! \delta_{ll'}, \quad l, l' = 0, 1, 2, \dots, \quad (3.2)$$

where $\delta_{ll'}$ is the Kronecker delta.

As in [6], we define the scaled Hermite functions

$$h_l(z) = e^{-\gamma_z z^2/2} H_l(\sqrt{\gamma_z} z) / \sqrt{2^l l!} (\gamma_z/\pi)^{1/4}, \quad z \in \mathbb{R}. \quad (3.3)$$

It is clear that $\lim_{|z| \rightarrow \infty} h_l(z) = 0$.

Plugging (3.3) into (3.1) and (3.2), a simple computation shows

$$B^z h_l(z) = -\frac{1}{2}h_l''(z) + \frac{1}{2}\gamma_z^2 z^2 h_l(z) = \left(l + \frac{1}{2}\right)\gamma_z h_l(z), \quad z \in \mathbb{R}, \quad l \geq 0, \quad (3.4)$$

$$\int_{-\infty}^{\infty} h_l(z)h_{l'}(z)dz = \delta_{ll'}, \quad l, l' = 0, 1, 2, \dots \quad (3.5)$$

Hence $\{h_l\}_{l=0}^{\infty}$ are eigenfunctions of the linear operator B^z in (1.4).

We now consider B_m^r . To this end, we recall the definition for the generalized-Laguerre polynomials.

For any fixed m ($m = 0, 1, 2, \dots$), let $\hat{L}_k^m(r)$ ($k = 0, 1, 2, \dots$) be the generalized-Laguerre polynomials of degree k satisfying [27]

$$\left(r \frac{d^2}{dr^2} + (m+1-r)\frac{d}{dr}\right) \hat{L}_k^m(r) + k\hat{L}_k^m(r) = 0, \quad k = 0, 1, 2, \dots, \quad (3.6)$$

$$\int_0^{\infty} r^m e^{-r} \hat{L}_k^m(r) \hat{L}_{k'}^m(r) dr = C_k^m \delta_{kk'}, \quad k, k' = 0, 1, 2, \dots, \quad (3.7)$$

where

$$C_k^m = \Gamma(m+1) \binom{k+m}{k} = \prod_{j=1}^m (k+j), \quad k = 0, 1, 2, \dots$$

We define the scaled generalized-Laguerre functions L_k^m by

$$L_k^m(r) = \frac{\gamma_r^{(m+1)/2}}{\sqrt{\pi C_k^m}} r^m e^{-\gamma_r r^2/2} \hat{L}_k^m(\gamma_r r^2). \quad (3.8)$$

Plugging (3.8) into (3.6) and (3.7), a tedious but simple computation (see detail in Appendix A) leads to

$$B_m^r L_k^m(r) = \left[-\frac{1}{2r} \frac{d}{dr} \left(r \frac{d}{dr} \right) + \frac{m^2}{2r^2} + \frac{1}{2} \gamma_r^2 r^2 \right] L_k^m(r) = \gamma_r (2k + m + 1) L_k^m(r), \quad (3.9)$$

$$2\pi \int_0^\infty L_k^m(r) L_{k'}^m(r) r dr = \delta_{kk'}. \quad (3.10)$$

Hence $\{L_k^m\}_{k=0}^\infty$ are eigenfunctions of B_m^r . We note that the basis functions $\{L_k^m\}_{k=0}^\infty$ with $m = 0$ were already used in [6].

Finally, we derive from the above that

$$\begin{aligned} B_m(L_k^m(r) h_l(z)) &= h_l(z) B_m^r L_k^m(r) + L_k^m(r) B^z h_l(z) \\ &= \gamma_r (2k + m + 1) L_k^m(r) h_l(z) + \gamma_z \left(l + \frac{1}{2} \right) L_k^m(r) h_l(z) \end{aligned} \quad (3.11)$$

$$= \left[\gamma_r (2k + m + 1) + \gamma_z \left(l + \frac{1}{2} \right) \right] L_k^m(r) h_l(z). \quad (3.12)$$

Hence, $\{L_k^m(r) h_l(z)\}_{k,l=0}^\infty$ are eigenfunctions of the operator B_m defined in (1.4).

3.2. Interpolation operators

In order to efficiently deal with the term $|\phi^n|^2 \tilde{\phi}^{n+1,p}$ in (2.14), a proper interpolation operator should be used. We shall define below scaled interpolation operators in both r, z directions and in the (r, z) space.

Let $\{\hat{z}_s\}_{s=0}^N$ be the Hermite–Gauss points, i.e., they are the $N + 1$ roots of the Hermite polynomial $H_{N+1}(z)$, and let $\{\hat{\omega}_s^z\}_{s=0}^N$ be the associated Hermite–Gauss quadrature weights [27]. We have

$$\sum_{s=0}^N \hat{\omega}_s^z \frac{H_l(\hat{z}_s)}{\pi^{1/4} \sqrt{2^l l!}} \frac{H_{l'}(\hat{z}_s)}{\pi^{1/4} \sqrt{2^{l'} l'!}} = \delta_{ll'}, \quad l, l' = 0, 1, \dots, N. \quad (3.13)$$

We then define the scaled Hermite–Gauss points and weights by

$$z_s = \frac{\hat{z}_s}{\sqrt{\gamma_z}}, \quad \omega_s^z = \frac{\hat{\omega}_s^z e^{\hat{z}_s^2}}{\sqrt{\gamma_z}}, \quad s = 0, 1, 2, \dots, N. \quad (3.14)$$

We derive from (3.3) and (3.13) that

$$\sum_{s=0}^N \omega_s^z h_l(z_s) h_{l'}(z_s) = \sum_{s=0}^N \frac{\hat{\omega}_s^z e^{\hat{z}_s^2}}{\sqrt{\gamma_z}} h_l(\hat{z}_s/\sqrt{\gamma_z}) h_{l'}(\hat{z}_s/\sqrt{\gamma_z}) = \sum_{s=0}^N \hat{\omega}_s^z \frac{H_l(\hat{z}_s)}{\pi^{1/4} \sqrt{2^l l!}} \frac{H_{l'}(\hat{z}_s)}{\pi^{1/4} \sqrt{2^{l'} l'!}} = \delta_{ll'}, \quad l, l' = 0, 1, \dots, N. \quad (3.15)$$

Let us denote

$$Y_N = \text{span}\{h_k : k = 0, 1, \dots, N\}. \quad (3.16)$$

We define

$$I_N^z : C(\mathbb{R}) \rightarrow Y_N \quad \text{such that } (I_N^z f)(z_s) = f(z_s), \quad s = 0, 1, \dots, N, \quad \forall f \in C(\mathbb{R}). \quad (3.17)$$

Now, let $\{\hat{r}_j^m\}_{j=0}^M$ be the generalized-Laguerre–Gauss points [27,26]; i.e. they are the $M + 1$ roots of the polynomial $\hat{L}_{M+1}^m(r)$, and let $\{\hat{\omega}_j^m\}_{j=0}^M$ be the weights associated with the generalized-Laguerre–Gauss quadrature [27,26]. Then, we have

$$\sum_{j=0}^M \hat{\omega}_j^m \frac{\hat{L}_k^m(\hat{r}_j^m)}{\sqrt{C_k^m}} \frac{\hat{L}_{k'}^m(\hat{r}_j^m)}{\sqrt{C_{k'}^m}} = \delta_{kk'}, \quad k, k' = 0, 1, \dots, M. \quad (3.18)$$

We then define the scaled generalized-Laguerre–Gauss points and weights by

$$r_j^m = \sqrt{\frac{\hat{r}_j^m}{\gamma_r}}, \quad \omega_j^m = \frac{\pi \hat{\omega}_j^m e^{\hat{r}_j^m}}{\gamma_r (\hat{r}_j^m)^m}, \quad j = 0, 1, \dots, M. \quad (3.19)$$

We derive from (3.8) and (3.18) that

$$\sum_{j=0}^M \omega_j^m L_k^m(r_j^m) L_{k'}^m(r_j^m) = \sum_{j=0}^M \frac{\pi \hat{\omega}_j^m e^{\hat{r}_j^m}}{\gamma_r (\hat{r}_j^m)^m} L_k^m \left(\sqrt{\hat{r}_j^m / \gamma_r} \right) L_{k'}^m \left(\sqrt{\hat{r}_j^m / \gamma_r} \right) = \sum_{j=0}^M \hat{\omega}_j^m \frac{\hat{L}_k^m(\hat{r}_j^m)}{\sqrt{C_k^m}} \frac{\hat{L}_{k'}^m(\hat{r}_j^m)}{\sqrt{C_{k'}^m}} = \delta_{kk'}, \quad k, k' = 0, 1, \dots, M. \quad (3.20)$$

Let us denote

$$X_M^m = \text{span}\{L_k^m : k = 0, 1, \dots, M\}. \quad (3.21)$$

We define

$$I_M^m : C(\overline{\mathbb{R}}_+) \rightarrow X_M^m \quad \text{such that } (I_M^m f)(r_j^m) = f(r_j^m), j = 0, 1, \dots, M, \quad \forall f \in C(\overline{\mathbb{R}}_+). \quad (3.22)$$

Finally, let

$$X_{MN}^m = \text{span}\{L_k^m(r)h_l(z) : k = 0, 1, 2, \dots, M, l = 0, 1, 2, \dots, N\}. \quad (3.23)$$

We define $I_{MN}^m : C(\overline{\mathbb{R}}_+ \times \mathbb{R}) \rightarrow X_{MN}^m$ such that

$$(I_{MN}^m f)(r_j^m, z_s) = f(r_j^m, z_s), \quad j = 0, 1, \dots, M, s = 0, 1, \dots, N, \forall f \in C(\overline{\mathbb{R}}_+ \times \mathbb{R}). \quad (3.24)$$

It is clear that $I_{MN}^m = I_M^m \circ I_N$.

Note that the computation of the weights $\{\omega_j^m, \omega_s^z\}$ from (3.19) and (3.14) is not a stable process for large m, M and N . However, they can be computed in a stable way as suggested in the Appendix of [26].

4. The generalized-Laguerre–Hermite pseudospectral methods

4.1. A Hermite pseudospectral method in 1D

In this section, we introduce a Hermite pseudospectral method for computing ground states of 1D BEC. In fact, when $\gamma_r \gg \gamma_z$ in (1.1), the 3D GPE (1.1) can be approximated by a 1D GPE [24,4]. In this case, the stationary states satisfy

$$\mu\phi = \left[-\frac{1}{2} \frac{\partial^2}{\partial z^2} + \frac{1}{2} \gamma_z^2 z^2 + W(z) + \beta_1 |\phi|^2 \right] \phi \quad (4.1)$$

under the normalization condition

$$\|\phi\|^2 = \int_{-\infty}^{\infty} |\phi(z)|^2 dz = 1, \quad (4.2)$$

where $\phi = \phi(z)$ and $\beta_1 \approx \beta\gamma_r/2\pi$ [4]. Any eigenvalue (or chemical potential) μ can be computed from its corresponding eigenfunction ϕ by

$$\mu = \int_{-\infty}^{\infty} \left[\frac{1}{2} |\partial_z \phi|^2 + \left(\frac{1}{2} \gamma_z^2 z^2 + W(z) \right) |\phi|^2 + \beta_1 |\phi|^4 \right] dz := \mu(\phi). \quad (4.3)$$

As described in Section 2, this nonlinear eigenvalue problem (4.1) can also be viewed as the Euler–Lagrangian equations of the energy functional $E(\phi)$, defined as

$$E(\phi) = \int_{-\infty}^{\infty} \left[\frac{1}{2} |\partial_z \phi|^2 + \left(\frac{1}{2} \gamma_z^2 z^2 + W(z) \right) |\phi|^2 + \frac{\beta_1}{2} |\phi|^4 \right] dz, \quad (4.4)$$

under the constraint (4.2). Similarly, in this case, the normalized gradient flow (2.3)–(2.7) collapses to

$$\frac{\partial}{\partial t} \phi(z, t) = -B^z \phi - W(z) \psi - \beta_1 |\phi|^2 \phi, \quad (4.5)$$

$$\lim_{|z| \rightarrow \infty} \phi(z, t) = 0, \quad t \geq 0, \quad (4.6)$$

$$\phi(z, t_{n+1}) := \phi(z, t_{n+1}^+) = \frac{\phi(z, t_{n+1}^-)}{\|\phi(\cdot, t_{n+1}^-)\|}, \quad (4.7)$$

$$\phi(z, 0) = \phi_0(z), \quad z \in \mathbb{R} \quad \text{with } \|\phi_0(\cdot)\| = 1, \quad (4.8)$$

where $\phi(z, t_n^\pm) = \lim_{t \rightarrow t_n^\pm} \phi(z, t)$, $\|\phi(\cdot)\|^2 = \int_{-\infty}^{\infty} |\phi(z)|^2 dz$.

Similarly, the scheme (2.14) in this case becomes:

$$\frac{\tilde{\phi}^{n+1,p+1}(z) - \phi^n(z)}{\Delta t} = -(B^z + \alpha_n) \tilde{\phi}^{n+1,p+1} + (\alpha_n - W(z) - \beta_1 |\phi^n|^2) \tilde{\phi}^{n+1,p}. \quad (4.9)$$

We now describe a pseudospectral method based on the scaled Hermite functions $\{h_i(z)\}$ for (4.19)–(2.15).

Let $(u, v)_\mathbb{R} = \int_{\mathbb{R}} uv dz$ and $\phi_N^0 \in Y_N$. For $n = 0, 1, \dots$, set $\tilde{\phi}_N^{n+1,0} = \phi_N^n$ and $\alpha_n = \frac{1}{2}(b_{\min}^n + b_{\max}^n)$ with

$$b_{\min}^n = \min_{-\infty < z < \infty} [W(z) + \beta_1 |\phi_N^n(z)|^2], \quad b_{\max}^n = \max_{-\infty < z < \infty} [W(z) + \beta_1 |\phi_N^n(z)|^2].$$

Then, the Hermite pseudospectral method for (4.19)–(2.15) is

Find $\tilde{\phi}_N^{n+1,p+1} \in Y_N$ such that

$$\left(\frac{\tilde{\phi}_N^{n+1,p+1} - \phi_N^n}{\Delta t} + (B^z + \alpha_n) \tilde{\phi}_N^{n+1,p+1}, h_l \right)_\mathbb{R} = \left(I_N^z [(\alpha_n - W - \beta_1 |\phi_N^n|^2) \tilde{\phi}_N^{n+1,p}], h_l \right)_\mathbb{R}, \quad 0 \leq l \leq N, \quad p = 0, 1, \dots, \quad (4.10)$$

$$\tilde{\phi}_N^{n+1} = \lim_{p \rightarrow \infty} \tilde{\phi}_N^{n+1,p}, \quad \phi_N^{n+1} = \frac{\tilde{\phi}_N^{n+1}}{\|\tilde{\phi}_N^{n+1}\|}.$$

We note that $\tilde{\phi}_N^{n+1,p+1}$ can be easily determined from (4.10) as follows:

We write the expansion

$$\tilde{\phi}_N^{n+1,p+1}(z) = \sum_{l=0}^N \hat{\phi}_l^{n+1,p+1} h_l(z), \quad \phi_N^n(z) = \sum_{l=0}^N \hat{\phi}_l^n h_l(z) \quad (4.11)$$

and

$$g^{n,p}(z) = I_N^z [(\alpha_n - W(z) - \beta_1 |\phi_N^n(z)|^2) \tilde{\phi}_N^{n+1,p}(z)] = \sum_{l=0}^N \hat{g}_l^{n,p} h_l(z),$$

where the coefficients $\{\hat{g}_l^{n,p}\}_{l=0}^N$ can be computed from the known function values $\{g^{n,p}(z_s)\}_{s=0}^N$ through the discrete Hermite transform using (3.15), i.e.

$$\hat{g}_l^{n,p} = \sum_{s=0}^N g^{n,p}(z_s) h_l(z_s) \omega_s^z. \quad (4.12)$$

Thanks to (3.4) and (3.5), we find from (4.10) that

$$\frac{\hat{\phi}_l^{n+1,p+1} - \hat{\phi}_l^n}{\Delta t} = - \left[\gamma_z \left(l + \frac{1}{2} \right) + \alpha_n \right] \hat{\phi}_l^{n+1,p+1} + \hat{g}_l^{n,p}, \quad l = 0, 1, \dots, N, \quad (4.13)$$

from which we derive

$$\hat{\phi}_l^{n+1,p+1} = \frac{\hat{\phi}_l^n + \Delta t \hat{g}_l^{n,p}}{1 + \Delta t [\alpha_n + \gamma_z (l + \frac{1}{2})]}, \quad l = 0, 1, \dots, N. \quad (4.14)$$

Then, $\tilde{\phi}_N^{n+1}$ and ϕ_N^{n+1} can be determined from the second equation in (4.10).

4.2. A generalized-Laguerre pseudospectral method in 2D

We now consider the 2D BEC with radial symmetry. The physical motivation is that when $\gamma_z \gg \gamma_r$ in (1.1), the 3D GPE (1.1) can be approximated by a 2D GPE [24]. In this case, the radial symmetric state ($m = 0$) and central vortex state with index m ($m \neq 0$) satisfy

$$\mu_m \phi_m = \frac{1}{2} \left[-\frac{1}{r} \frac{\partial}{\partial r} \left(r \frac{\partial}{\partial r} \right) + \gamma_r^2 r^2 + \frac{m^2}{r^2} + 2\beta_2 |\phi_m|^2 \right] \phi_m, \quad (4.15)$$

$$\phi_m(0) = 0 \quad (\text{for } m \neq 0), \quad \lim_{r \rightarrow \infty} \phi_m(r) = 0, \quad (4.16)$$

under the normalization condition

$$\|\phi_m\|^2 = 2\pi \int_0^\infty |\phi_m(r)|^2 r dr = 1, \quad (4.17)$$

where $\phi_m = \phi_m(r)$ and $\beta_2 \approx \beta \sqrt{\gamma_z/2\pi}$ [4]. Any eigenvalue (or chemical potential) μ_m can be computed from its corresponding eigenfunction ϕ_m by

$$\mu_m = \pi \int_0^\infty \left[|\partial_r \phi_m|^2 + \left(\gamma_r^2 r^2 + \frac{m^2}{r^2} \right) |\phi_m|^2 + 2\beta_2 |\phi_m|^4 \right] r dr := \mu(\phi_m). \quad (4.18)$$

Again, this nonlinear eigenvalue problem (4.15)–(4.17) can also be viewed as the Euler–Lagrangian equations of the energy functional $E(\phi_m)$, defined by

$$E(\phi_m) = \pi \int_0^\infty \left[|\partial_r \phi_m|^2 + \left(\gamma_r^2 r^2 + \frac{m^2}{r^2} \right) |\phi_m|^2 + \beta_2 |\phi_m|^4 \right] r dr, \quad (4.19)$$

under the constraint (4.17). Accordingly, the normalized gradient flow (2.3)–(2.7) collapses to

$$\frac{\partial}{\partial t} \phi(r, t) = -B_m^r \phi - \beta_2 |\phi|^2 \phi, \quad (4.20)$$

$$\phi(0, t) = 0 \quad (\text{for } m \neq 0), \quad \lim_{r \rightarrow \infty} \phi(r, t) = 0, \quad t \geq 0, \quad (4.21)$$

$$\phi(r, t_{n+1}) := \phi(r, t_{n+1}^+) = \frac{\phi(r, t_{n+1}^-)}{\|\phi(\cdot, t_{n+1}^-)\|}, \quad (4.22)$$

$$\phi(r, 0) = \phi_0(r), \quad 0 \leq r < \infty, \quad \text{with } \|\phi_0(\cdot)\| = 1, \quad (4.23)$$

where $\phi(r, t_n^\pm) = \lim_{t \rightarrow t_n^\pm} \phi(r, t)$, $\|\phi(\cdot)\|^2 = 2\pi \int_0^\infty |\phi(r)|^2 r dr$. The scheme (2.14) in this case becomes:

$$\frac{\tilde{\phi}^{n+1,p+1} - \phi^n(r)}{\Delta t} = -(B_m^r + \alpha_n) \tilde{\phi}^{n+1,p+1} + (\alpha_n - \beta_2 |\phi^n|^2) \tilde{\phi}^{n+1,p}. \quad (4.24)$$

We now describe a pseudospectral method based on the scaled generalized-Laguerre functions $\{L_k^m(r)\}$ for (4.24)–(2.15).

Let $(u, v)_{r, \mathbb{R}_+} = \int_{\mathbb{R}_+} u v r dr$ and $\phi_M^0 \in X_M^m$. For $n = 0, 1, \dots$, set $\tilde{\phi}_M^{n+1,0} = \phi_M^n$ and $\alpha_n = \frac{1}{2}(b_{\min}^n + b_{\max}^n)$ with

$$b_{\min}^n = \min_{0 \leq r < \infty} [\beta_2 |\phi_M^n(r)|^2], \quad b_{\max}^n = \max_{0 \leq r < \infty} [\beta_2 |\phi_M^n(r)|^2].$$

Then, the generalized-Laguerre pseudospectral method for (4.24)–(2.15) is

find $\tilde{\phi}_M^{n+1,p+1} \in X_M^m$ such that

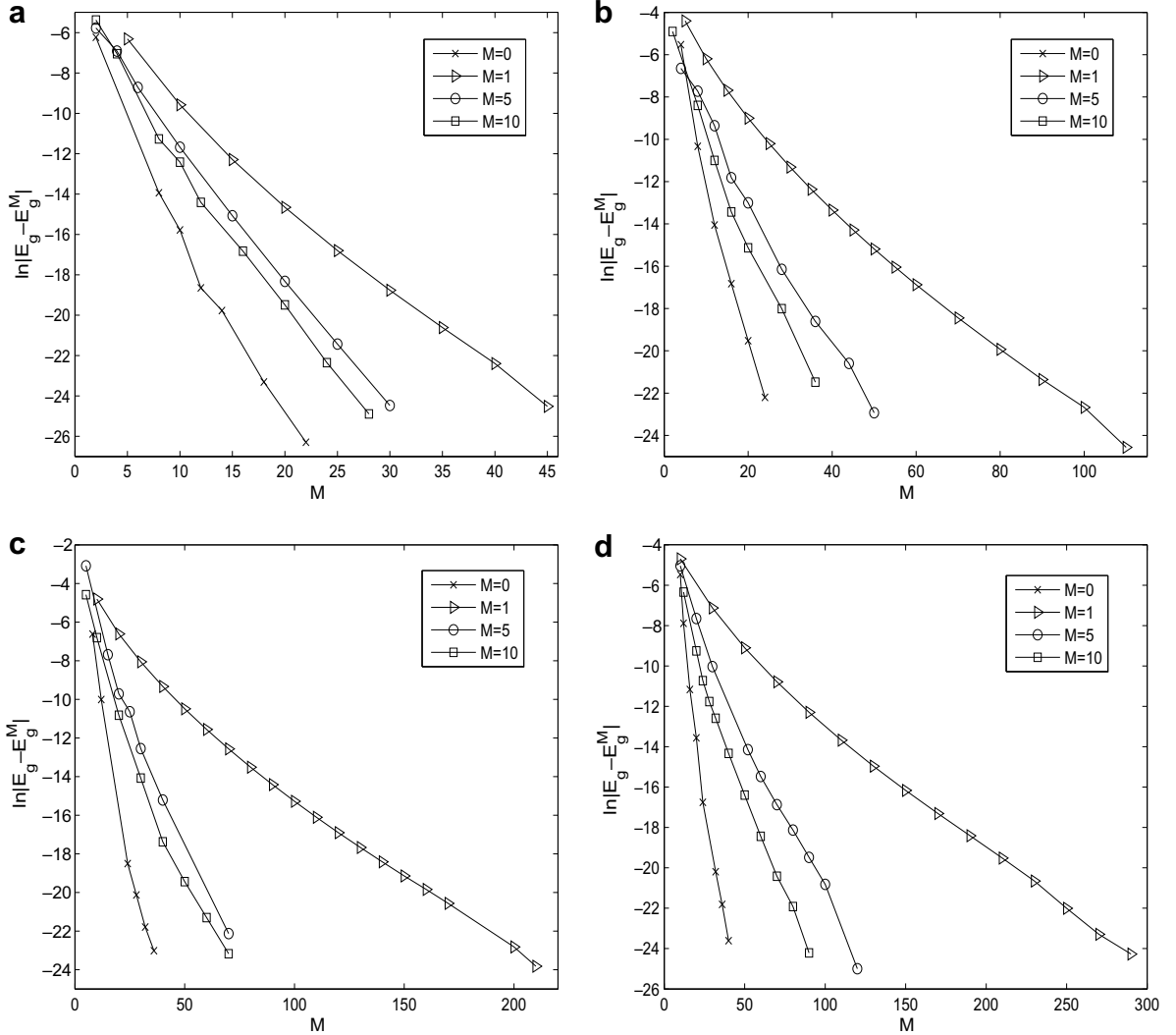


Fig. 1. Error analysis for computing symmetric and central vortex states of 2D BEC with radial symmetry by using (4.25) for different m and β_2 : (a) $\beta_2 = 10$; (b) $\beta_2 = 100$; (c) $\beta_2 = 500$ and (d) $\beta_2 = 1000$.

$$\left(\frac{\tilde{\phi}_M^{n+1,p+1} - \phi_M^n}{\Delta t} + (B_m^r + \alpha_n) \tilde{\phi}_M^{n+1,p+1}, L_k^m \right)_{r,\mathbb{R}_+} = \left(I_M^m [(\alpha_n - \beta_2 |\phi_M^n|^2) \tilde{\phi}_M^{n+1,p}], L_k^m \right)_{r,\mathbb{R}_+}, \quad 0 \leq k \leq M, \quad p = 0, 1, \dots, \quad (4.25)$$

$$\tilde{\phi}_M^{n+1} = \lim_{p \rightarrow \infty} \tilde{\phi}_M^{n+1,p}, \quad \phi_M^{n+1} = \frac{\tilde{\phi}_M^{n+1}}{\|\tilde{\phi}_M^{n+1}\|}.$$

The function $\tilde{\phi}_M^{n+1,p+1}$ can be easily determined from (4.25) as follows:

We write the expansion

$$\tilde{\phi}_M^{n+1,p+1}(r) = \sum_{k=0}^M \hat{\phi}_k^{n+1,p+1} L_k^m(r), \quad \phi_M^n(r) = \sum_{k=0}^M \hat{\phi}_k^n L_k^m(r) \quad (4.26)$$

Table 1

Radius mean square σ_r , energy $E_g = E(\phi_m^M)$ and chemical potential $\mu_g = \mu(\phi_m^M)$ of the symmetric and central vortex states of 2D BEC with radial symmetry and $M = 50$ for $\beta_2 = 10$ with different index m

m	σ_r	$E_g = E(\phi_m^M)$	$\mu_g = \mu(\phi_m^M)$
0	1.26187099	1.59231902	2.06375207
1	1.53661556	2.36118811	2.69167784
2	1.81131962	3.28087973	3.54606849
3	2.05852636	4.23753202	4.46481551
4	2.28243553	5.20951367	5.41148881
5	2.48787557	6.18952687	6.37311430
6	2.67849796	7.17435364	7.34381582
7	2.85697868	8.16233006	8.32050594
8	3.02530922	9.15249908	9.30138980
9	3.18500597	10.14426648	10.28534445
10	3.33724995	11.13724135	11.27162695
15	4.01410239	16.11302510	16.22417440
20	4.59329096	21.09833182	21.19526717
25	5.10766022	26.08820593	26.17529928
30	5.57500370	31.08068376	31.16044271
40	6.40859067	41.07006163	41.13943156
50	7.14581945	51.06277304	51.12499344
60	7.81391854	61.05737347	61.11428672
70	8.42930019	71.05316613	71.10593791

Table 2

Radius mean square σ_r , energy $E_g = E(\phi_m^M)$ and chemical potential $\mu_g = \mu(\phi_m^M)$ of the symmetric and central vortex states of 2D BEC with radial symmetry with $M = 50$ for $\beta_2 = 1000$ with different index m

m	σ_r	$E_g = E(\phi_m^M)$	$\mu_g = \mu(\phi_m^M)$
0	3.46002488	11.97177422	17.88864690
1	3.48804397	12.16645295	18.01329019
2	3.54187594	12.54488754	18.28085868
3	3.61096998	13.03908997	18.65105895
4	3.68987248	13.61513463	19.10081655
5	3.77523196	14.25239728	19.61440987
6	3.86485616	14.93711583	20.18040284
7	3.95722132	15.65959765	20.79002576
8	4.05126566	16.41275862	21.43646734
9	4.14623407	17.19126236	22.11432074
10	4.24157906	17.99099505	22.81921308
15	4.71325107	22.21474032	26.64340068
20	5.16463355	26.67344552	30.79661542
25	5.59169606	31.26707242	35.14839763
30	5.99555631	35.94670464	39.63069139
40	6.74285862	45.46615497	48.84438714
50	7.42403523	55.11631738	58.26543378
60	8.05269647	64.84594441	67.81460909
70	8.63876455	74.62828335	77.44968607

and

$$g^{n,p}(z) = I_M^m[(\alpha_n - \beta_2 |\phi_M^n(r)|^2) \tilde{\phi}_M^{n+1,p}(r)] = \sum_{k=0}^M \hat{g}_k^{n,p} L_k^m(r),$$

where the coefficients $\{\hat{g}_k^{n,p}\}_{k=0}^M$ can be computed from the known function values $\{g^{n,p}(r_j^m)\}_{j=0}^M$ through the discrete generalized-Laguerre transform using (3.20), i.e.,

$$\hat{g}_k^{n,p} = \sum_{j=0}^M g^{n,p}(r_j^m) L_k^m(r_j^m) \omega_j^r. \quad (4.27)$$

Thanks to (3.9) and (3.10), we find from (4.25) that

$$\frac{\hat{\phi}_k^{n+1,p+1} - \hat{\phi}_k^n}{\Delta t} = -[\gamma_r(2k + m + 1) + \alpha_n] \hat{\phi}_k^{n+1,p+1} + \hat{g}_k^{n,p}, \quad k = 0, 1, \dots, N, \quad (4.28)$$

from which we derive

$$\hat{\phi}_k^{n+1,p+1} = \frac{\hat{\phi}_k^n + \Delta t \hat{g}_k^{n,p}}{1 + \Delta t [\alpha_n + \gamma_r(2k + m + 1)]}, \quad k = 0, 1, \dots, N. \quad (4.29)$$

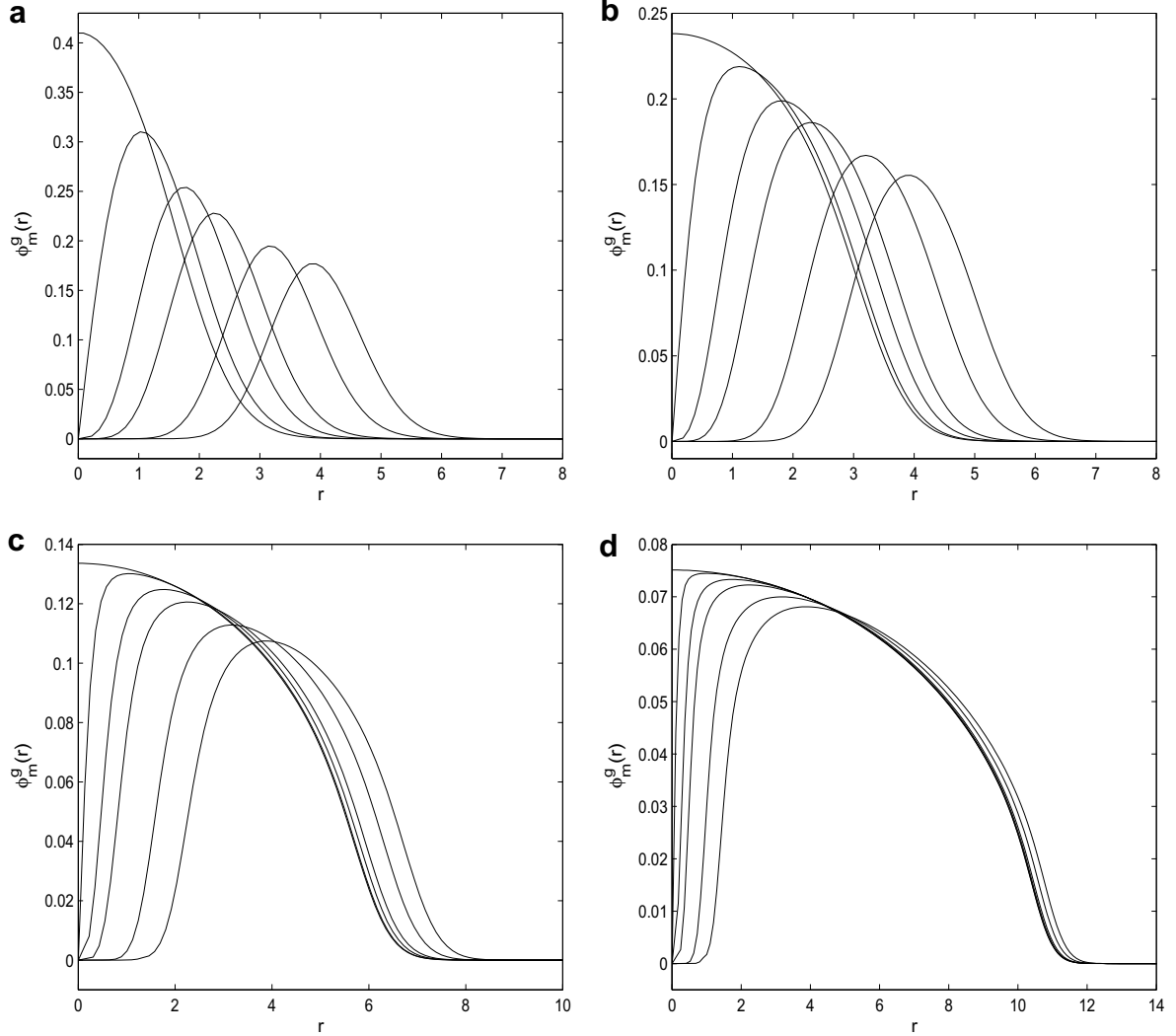


Fig. 2. Symmetric and central vortex states of 2D BEC with radial symmetry for $m = 0, 1, 3, 5, 10, 15$ (in the order of decreasing of peak values) and different β_2 : (a) $\beta_2 = 10$; (b) $\beta_2 = 100$; (c) $\beta_2 = 1000$ and (d) $\beta_2 = 10,000$.

Then, $\tilde{\phi}_M^{n+1}$ and ϕ_M^{n+1} can be determined from the second equation in (4.25).

4.3. A generalized-Laguerre–Hermite pseudospectral method in 3D

We are now in position to describe the generalized-Laguerre–Hermite pseudospectral method for computing symmetric and central vortex line states of 3D BEC with cylindrical symmetry.

Let $(u, v)_{r, \mathbb{R}_+ \times \mathbb{R}} = \int_{\mathbb{R}} \int_{\mathbb{R}_+} u v r dr dz$ and $\phi_{MN}^0 \in X_{MN}^m$. For $n = 0, 1, \dots$, set $\tilde{\phi}_{MN}^{n+1,0} = \phi_{MN}^n$ and $\alpha_n = \frac{1}{2}(b_{\min}^n + b_{\max}^n)$ with

$$b_{\min}^n = \min_{(r,z) \in \mathbb{R}_+ \times \mathbb{R}} [W(z) + \beta |\phi_{MN}^n(r, z)|^2], \quad b_{\max}^n = \max_{(r,z) \in \mathbb{R}_+ \times \mathbb{R}} [W(z) + \beta |\phi_{MN}^n(r, z)|^2].$$

Then, the generalized-Laguerre–Hermite pseudospectral method for (2.14), (2.15) is: find $\tilde{\phi}_{MN}^{n+1,p+1} \in X_{MN}^m$ such that for $0 \leq k \leq M, 0 \leq l \leq N, p = 0, 1, \dots$,

$$\left(\frac{\tilde{\phi}_{MN}^{n+1,p+1} - \phi_{MN}^n}{\Delta t} + (B_m + \alpha_n) \tilde{\phi}_{MN}^{n+1,p+1}, L_k^m(r) h_l(z) \right)_{r, \mathbb{R}_+ \times \mathbb{R}} = \left(I_{MN}^m[(\alpha_n - W(z) - \beta |\phi_{MN}^n|^2) \tilde{\phi}_{MN}^{n+1,p}], L_k^m(r) h_l(z) \right)_{r, \mathbb{R}_+ \times \mathbb{R}}, \quad (4.30)$$

$$\tilde{\phi}_{MN}^{n+1} = \lim_{p \rightarrow \infty} \tilde{\phi}_{MN}^{n+1,p}, \quad \phi_{MN}^{n+1} = \frac{\tilde{\phi}_{MN}^{n+1}}{\|\tilde{\phi}_{MN}^{n+1}\|}.$$

The function $\tilde{\phi}_{MN}^{n+1,p+1}$ can be easily determined from (4.30) as follows:

We write the expansion

$$\tilde{\phi}_{MN}^{n+1,p+1}(r, z) = \sum_{k=0}^M \hat{\phi}_{kl}^{n+1,p+1} L_k^m(r) h_l(z), \quad \phi_{MN}^n(r) = \sum_{k=0}^M \sum_{l=0}^N \hat{\phi}_{kl}^n L_k^m(r) h_l(z), \quad (4.31)$$

and

$$g^{n,p}(r, z) = I_{MN}^m[(\alpha_n - W(z) - \beta |\phi_{MN}^n(r, z)|^2) \tilde{\phi}_{MN}^{n+1,p}(r, z)] = \sum_{k=0}^M \sum_{l=0}^N \hat{g}_{kl}^{n,p} L_k^m(r) h_l(z),$$

where the coefficients $\{\hat{g}_{kl}^{n,p}\}$ can be computed from the known function values $\{g^{n,p}(r_j^m, z_s)\}$ through the discrete generalized-Laguerre transform and discrete Hermite transform using (3.20) and (3.15), i.e.,

$$\hat{g}_{kl}^{n,p} = \sum_{s=0}^N \sum_{j=0}^M g^{n,p}(r_j^m, z_s) L_k^m(r_j^m) h_l(z_s) \omega_j^r \omega_s^z. \quad (4.32)$$

Thanks to (3.9) and (3.10) and (3.4) and (3.5), we find from (4.30) that

$$\frac{\hat{\phi}_{kl}^{n+1,p+1} - \hat{\phi}_{kl}^n}{\Delta t} = - \left[\gamma_r (2k + m + 1) \gamma_z \left(l + \frac{1}{2} \right) + \alpha_n \right] \hat{\phi}_{kl}^{n+1,p+1} + \hat{g}_{kl}^{n,p}, \quad (4.33)$$

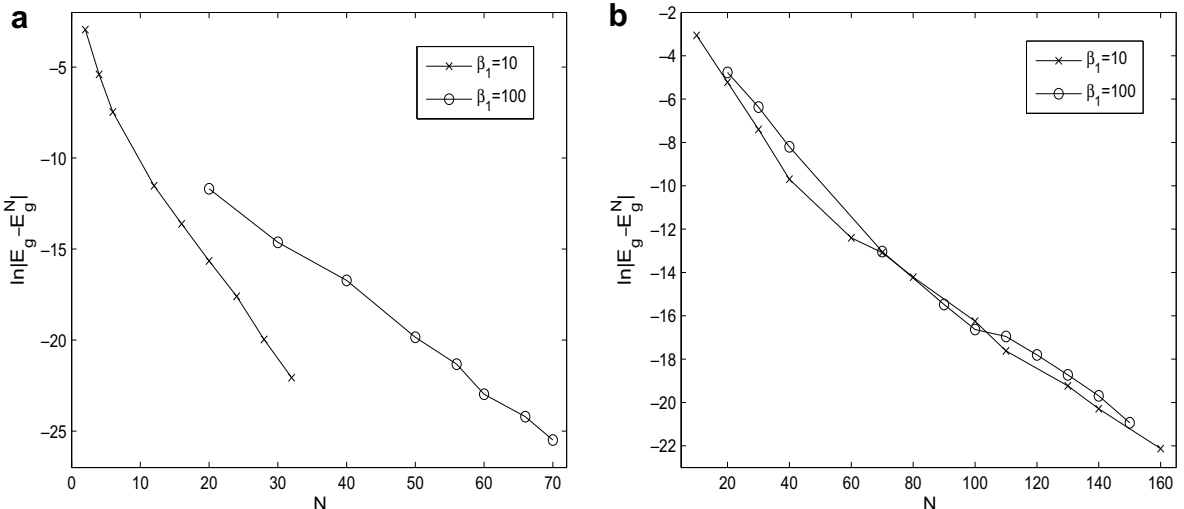


Fig. 3. Error analysis for computing ground states of 1D BEC with $W(z) = V_0 \sin^2(\pi z/4)$ by using (4.10) for different β_1 and V_0 : (a) $V_0 = 0$ and (b) $V_0 = 25$.

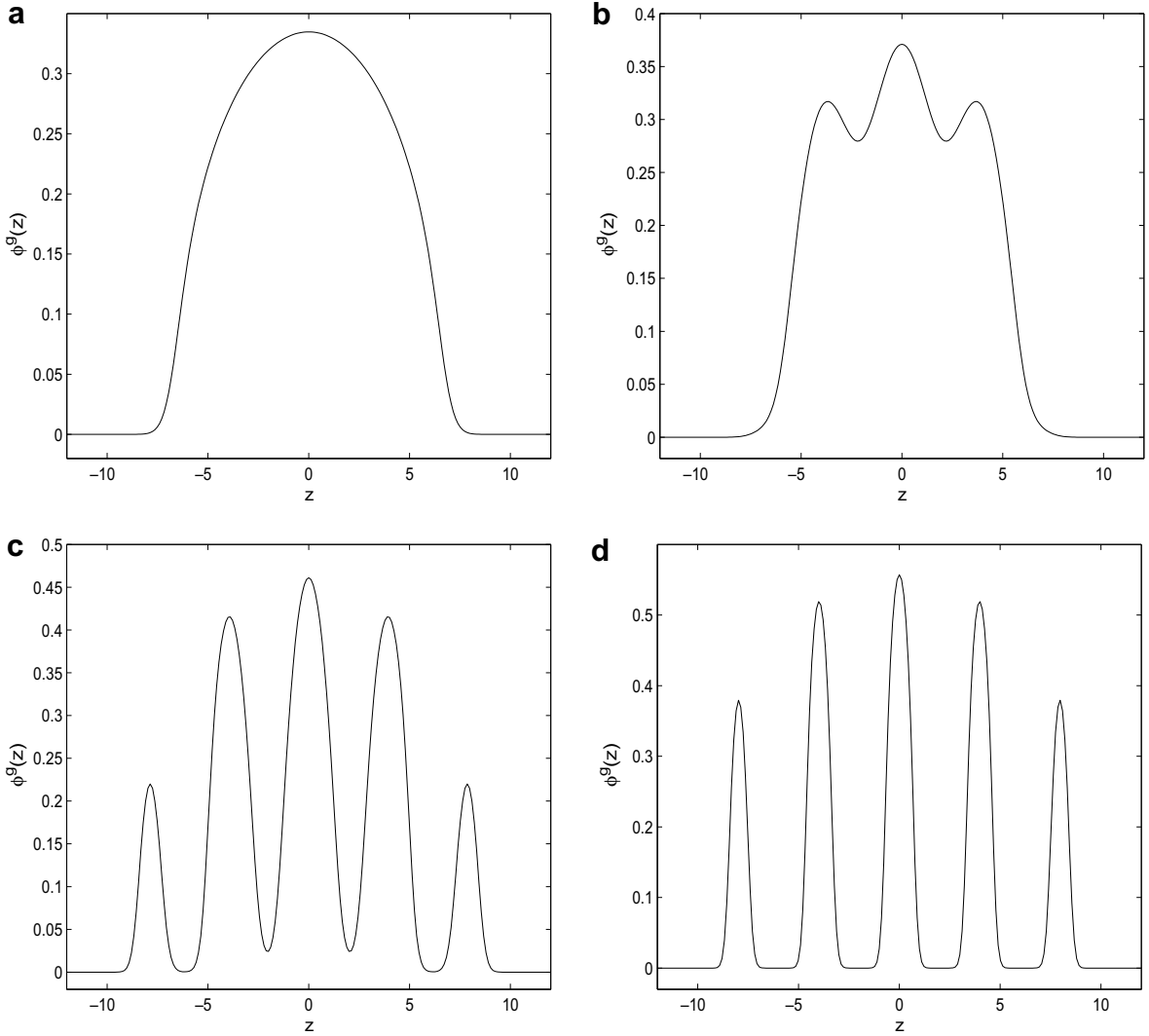


Fig. 4. Ground states of 1D BEC with $\beta_1 = 200$ and $W(z) = V_0 \sin^2(\pi z/4)$ for different V_0 : (a) $V_0 = 0$; (b) $V_0 = 10$; (c) $V_0 = 50$ and (d) $V_0 = 200$.

from which we derive

$$\hat{\phi}_{kl}^{n+1,p+1} = \frac{\hat{\phi}_{kl}^n + \Delta t g_{kl}^{n,p}}{1 + \Delta t [\alpha_n + \gamma_r(2k+m+1) + \gamma_z(l+\frac{1}{2})]}. \quad (4.34)$$

Then, $\tilde{\phi}_{MN}^{n+1}$ and ϕ_{MN}^{n+1} can be determined from the second equation in (4.30).

5. Numerical results

We now present some numerical results by using the numerical methods introduced in previous sections to demonstrate the spectral accuracy of the methods and to compute symmetric and central vortex states in BEC. To quantify the numerical results of a state $\phi(\mathbf{x})$ with $\|\phi(\cdot)\|^2 = \int_{\mathbb{R}^d} |\phi(\mathbf{x})|^2 d\mathbf{x} = 1$, we define the condensate widths along the r - and z -axes as σ_r and σ_z by

$$\sigma_\alpha^2 = \int_{\mathbb{R}^d} \alpha^2 |\phi(\mathbf{x})|^2 d\mathbf{x}, \quad \alpha = x, y, z; \quad \sigma_r^2 = \sigma_x^2 + \sigma_y^2. \quad (5.1)$$

Example 1. Symmetric and central vortex states of 2D BEC with radial symmetry, i.e. we take $\gamma_r = 1$ in (4.20).

We solve the problem by the scheme (4.25) with time step $\Delta t = 0.1$. Let $\phi_m^g(r)$ be the numerical ‘exact’ symmetric or central vortex state which is obtained numerically by using $M = 300$ in (4.25) and denote its energy as $E_g = E(\phi_m^g)$. Similarly,

let $\phi_m^M(r)$ be the numerical solution of the symmetric or central vortex state which is obtained numerically by (4.25) and denote its energy as $E_g^M = E(\phi_m^M)$. Fig. 1 plots the errors $\ln|E_g - E_g^M|$ vs. M for different m and β_2 . In addition, Table 1 lists radius mean square σ_r , energy $E(\phi_m^M)$ and chemical potential $\mu(\phi_m^M)$ with $M = 50$ and $\beta_2 = 10$ for different m , and Table 2 lists similar results for $\beta_2 = 1000$. Fig. 2 depicts $\phi_m^g(r)$ for different m and β_2 .

From Figs. 1 and 2, Tables 1 and 2 and additional numerical results not shown here for brevity, we can draw the following conclusions for our numerical method and the symmetric and central vortex states of 2D BEC with radial symmetry: (i) the scheme (4.25) is spectrally accurate for computing symmetric and central vortex states of 2D BEC with radial symmetry (cf. Fig. 1); (ii) for fixed β_2 , when the index m increases, the radius mean square σ_r , energy per particle E_g , chemical potential μ_g and vortex core size r_c (distance between the origin and the position where $\phi_m^g(r)$ attains its peak value) increase (cf. Tables 1, 2, Fig. 2); (iii) for fixed m , when β_2 increases, the radius mean square σ_r , energy per particle E_g and chemical potential μ_g increase, but the vortex core size r_c decreases and (iv) for any fixed $\beta_2 \geq 0$, we have

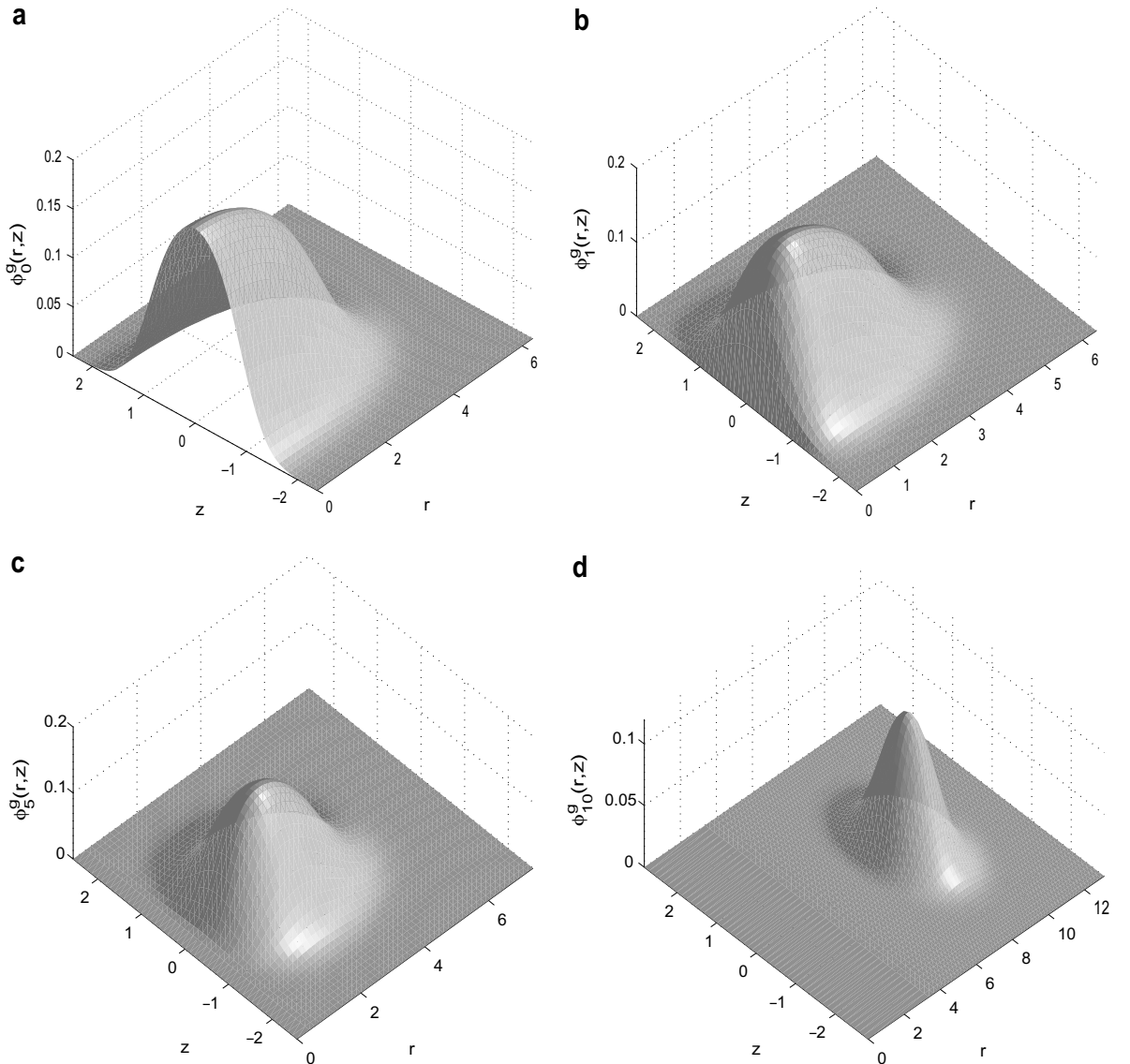


Fig. 5. Symmetric and central vortex line states of 3D BEC with cylindrical symmetry with $\gamma_r = 1$, $\gamma_z = 4$, $W(z) \equiv 0$ and $\beta = 200$ for different m : (a) $m = 0$; (b) $m = 1$; (c) $m = 5$ and (d) $m = 10$.

Table 3

Radius mean square σ_r and σ_z , energy $E_g = E(\phi_m^g)$ and chemical potential $\mu_g = \mu(\phi_m^g)$ of the symmetric and central vortex line states of 3D BEC with cylindrical symmetry for $\beta = 200$ with different index m

m	σ_r	σ_z	$E_g = E(\phi_m^g)$	$\mu_g = \mu(\phi_m^g)$
0	2.06682393	0.452574559	6.55486039	8.54323597
1	2.16965987	0.446595216	6.95925961	8.83813666
2	2.3204757	0.440390694	7.60644575	9.36924565
3	2.48315265	0.435085574	8.36376363	10.0262063
4	2.64661629	0.430634629	9.18307689	10.7606954
5	2.80687303	0.426872062	10.0414999	11.5470093
6	2.96249246	0.423650384	10.9265064	12.3699915
7	3.11305802	0.420856913	11.8305741	13.2200656
8	3.25861254	0.418405487	12.748872	14.0908206
9	3.3993583	0.416232548	13.6781349	14.9778097
10	3.53559224	0.414288234	14.6160647	15.8778101
15	4.15911019	0.406919394	19.3895928	20.5066343
20	4.70805515	0.401912034	24.2422615	25.2600451
25	5.20285443	0.398207476	29.1360907	30.0799082
30	5.65646951	0.395313022	34.0546463	34.940335
40	6.47197512	0.391006775	43.9357019	44.7343135
50	7.19779494	0.387893321	53.851271	54.5864518
60	7.85800817	0.385497866	63.7871598	64.4732469
70	8.46758734	0.38357611	73.736239	74.3827466

$$E(\phi_0^g) < E(\phi_1^g) < \dots < E(\phi_m^g) < \dots \Rightarrow \mu(\phi_0^g) < \mu(\phi_1^g) < \dots < \mu(\phi_m^g) < \dots,$$

$$E(\phi_{m+1}^g) \approx E(\phi_m^g) + 1, \quad \mu(\phi_{m+1}^g) \approx \mu(\phi_m^g) + 1, \quad m \gg 1,$$

$$\lim_{m \rightarrow \infty} \frac{E(\phi_m^g)}{\mu(\phi_m^g)} = 1.$$

Example 2. Ground state of 1D BEC, i.e. we take $\gamma_z = 1$, $W(z) = V_0 \sin^2(\pi z/4)$ with V_0 a constant in (4.5).

We solve the problem by the scheme (4.10) with time step $\Delta t = 0.1$. Let $\phi^g(z)$ be the numerical ‘exact’ ground state which is obtained numerically by using $N = 200$ in (4.10) and denote its energy as $E_g = E(\phi^g)$. Similarly, let $\phi^N(z)$ be the numerical solution of the ground state which is obtained by (4.10) and denote its energy as $E_g^N = E(\phi^N)$. Fig. 3 plots the errors $\ln |E_g - E_g^N|$ vs. N for different β_1 and V_0 . In addition, Fig. 4 depicts $\phi^g(z)$ with $\beta_1 = 200$ for different V_0 . The results in Fig. 3 demonstrates the spectral accuracy of the method (4.10) for computing ground state of 1D BEC.

Example 3. Symmetric and central vortex line states of 3D BEC with cylindrical symmetry, i.e. we take $\gamma_r = 1$, $\gamma_z = 4$ and $W(z) \equiv 0$ in (2.3).

We solve the problem by the scheme (4.30) with time step $\Delta t = 0.1$. Let $\phi_m^g(r, z)$ be the numerical solution of the symmetric or central vortex state which is obtained numerically with $M = 60$ and $N = 60$ in (4.30). Fig. 5 depicts $\phi_m^g(r, z)$ with $\beta = 200$ for different m . In addition, Table 3 lists radius mean square σ_r and σ_z , energy $E(\phi_m^g)$ and chemical potential $\mu(\phi_m^g)$ with $\beta_2 = 200$ for different m .

From Fig. 5, Table 3 and additional numerical results not shown here for brevity, we can draw the following conclusions for the symmetric and central vortex line states of 3D BEC with cylindrical symmetry: (i) for fixed β , when the index m increases, the radius mean square in r -direction σ_r , energy per particle E_g , chemical potential μ_g and vortex core size r_c increase (cf. Table 3 and Fig. 5), but the radius mean square in z -direction σ_z decreases (cf. Table 3); (ii) for fixed m , when β increases, the radius mean square σ_r and σ_z , energy per particle E_g and chemical potential μ_g increase, but the vortex core size r_c decreases; (iii) for any fixed $\beta \geq 0$, we have

$$E(\phi_0^g) < E(\phi_1^g) < \dots < E(\phi_m^g) < \dots \Rightarrow \mu(\phi_0^g) < \mu(\phi_1^g) < \dots < \mu(\phi_m^g) < \dots,$$

$$E(\phi_{m+1}^g) \approx E(\phi_m^g) + 1, \quad \mu(\phi_{m+1}^g) \approx \mu(\phi_m^g) + 1, \quad m \gg 1,$$

$$\lim_{m \rightarrow \infty} \frac{E(\phi_m^g)}{\mu(\phi_m^g)} = 1.$$

6. Concluding remarks

We developed in this paper a new generalized-Laguerre–Hermite pseudospectral method for computing symmetric and central vortex line states of 3D BEC with cylindrical symmetry. The new method takes advantage of the cylindrical symmetry so that only an effectively 2D problem needs to be solved. The method is based on appropriately scaled generalized-Laguerre–Hermite functions and the backward Euler time integrator for the normalized gradient flow. Hence it is spectrally accurate in space and very stable and efficient in practical computation for all $m \geq 0$. In fact, the method can be easily extended to compute symmetric and central vortex states in rotating BEC [8], multi-component BEC [31] and spin-1 BEC [7,5].

Acknowledgments

W.B. acknowledges support from Ministry of Education of Singapore Grant No. R-158-000-002-112. J.S. acknowledges support from NSF DMS-0610646. This work was partially done while the authors were visiting the Institute for Mathematical Sciences of National University of Singapore in 2007.

Appendix A. Derivation of (3.9) and (3.10)

When $m = 0$, (3.9) and (3.10) were derived in [6]. For any fixed $m \neq 0$, letting $z = \gamma_r r^2$ and differentiating (3.8) with respect to r , we obtain

$$\frac{d}{dr} L_k^m(r) = \frac{\gamma_r^{(m+1)/2}}{\sqrt{\pi C_k^m}} e^{-z/2} \left[r^{m-1} (m - \gamma_r r^2) \hat{L}_k^m(z) + 2\gamma_r r^{m+1} \frac{d}{dz} \hat{L}_k^m(z) \right]. \quad (\text{A.1})$$

Multiplying r at the both sides of (A.1) and then differentiating with respect to r , we get

$$\begin{aligned} \frac{d}{dr} \left(r \frac{d}{dr} L_k^m(r) \right) &= \frac{\gamma_r^{(m+1)/2}}{\sqrt{\pi C_k^m}} e^{-z/2} \left[\gamma_r r^{m+1} (\gamma_r r^2 - m) \hat{L}_k^m(z) - 2\gamma_r^2 r^{m+3} \frac{d}{dz} \hat{L}_k^m(z) \right. \\ &\quad + r^{m-1} (m^2 - (m+2)\gamma_r r^2) \hat{L}_k^m(z) + 2\gamma_r^2 r^{m+3} \frac{d^2}{dz^2} \hat{L}_k^m(z) \\ &\quad \left. + \gamma_r r^{m+1} (m - \gamma_r r^2) \frac{d}{dz} \hat{L}_k^m(z) + 2(m+2)\gamma_r r^{m+1} \frac{d}{dz} \hat{L}_k^m(z) \right] \\ &= \frac{\gamma_r^{(m+1)/2}}{\sqrt{\pi C_k^m}} e^{-z/2} \left[r^{m-1} (\gamma_r^2 r^4 - 2\gamma_r (m+1)r^2 + m^2) \hat{L}_k^m(z) \right. \\ &\quad \left. + 4\gamma_r r^{m+1} (m+1 - \gamma_r r^2) \frac{d}{dz} \hat{L}_k^m(z) + 4\gamma_r^2 r^{m+3} \frac{d^2}{dz^2} \hat{L}_k^m(z) \right] \\ &= \frac{z^{(m+1)/2}}{\sqrt{\pi C_k^m}} e^{-z/2} \left[\left(\gamma_r^2 r^2 - 2\gamma_r (m+1) + \frac{m^2}{r^2} \right) \hat{L}_k^m(z) + 4\gamma_r \left((m+1-z) \frac{d}{dz} \hat{L}_k^m(z) + z \frac{d^2}{dz^2} \hat{L}_k^m(z) \right) \right]. \end{aligned} \quad (\text{A.2})$$

Plugging (A.2) into the left hand of (3.9), noticing (3.6), we have

$$\begin{aligned} &- \frac{1}{2r} \frac{dL_k^m(r)}{dr} \left(r \frac{d}{dr} \right) + \left(\frac{m^2}{2r^2} + \frac{1}{2}\gamma_r^2 r^2 \right) L_k^m(r) \\ &= - \frac{\gamma_r^{1/2} z^{m/2}}{2\sqrt{\pi C_k^m}} e^{-z/2} \left[\left(\gamma_r^2 r^2 - 2\gamma_r (m+1) + \frac{m^2}{r^2} \right) \hat{L}_k^m(z) + 4\gamma_r \left((m+1-z) \frac{d}{dz} \hat{L}_k^m(z) + z \frac{d^2}{dz^2} \hat{L}_k^m(z) \right) \right] \\ &\quad + \left(\frac{m^2}{2r^2} + \frac{1}{2}\gamma_r^2 r^2 \right) \frac{\gamma_r^{1/2} z^{m/2}}{\sqrt{\pi C_k^m}} e^{-z/2} \hat{L}_k^m(z) \\ &= - \frac{\gamma_r^{1/2} z^{m/2}}{2\sqrt{\pi C_k^m}} e^{-z/2} \left[-2\gamma_r (m+1) \hat{L}_k^m(z) - 4\gamma_r k \hat{L}_k^m(z) \right] \\ &= \gamma_r (2k+m+1) L_k^m(r). \end{aligned} \quad (\text{A.3})$$

Similarly, plugging (3.8) into (3.10), noticing (3.7), we obtain

$$\begin{aligned} &2\pi \int_0^\infty L_k^m(r) L_{k'}^m(r) r dr \\ &= 2\pi \int_0^\infty \frac{\gamma_r^{(m+1)/2}}{\sqrt{\pi C_k^m}} r^m e^{-\gamma_r r^2/2} \hat{L}_k^m(\gamma_r r^2) \frac{\gamma_r^{(m+1)/2}}{\sqrt{\pi C_{k'}^m}} r^m e^{-\gamma_r r^2/2} \hat{L}_{k'}^m(\gamma_r r^2) r dr \\ &= \frac{1}{\sqrt{C_k^m C_{k'}^m}} \int_0^\infty (\gamma_r r^2)^m \hat{L}_k^m(\gamma_r r^2) \hat{L}_{k'}^m(\gamma_r r^2) d(\gamma_r r^2) \\ &= \frac{1}{\sqrt{C_k^m C_{k'}^m}} \int_0^\infty z^m \hat{L}_k^m(z) \hat{L}_{k'}^m(z) dz = \frac{1}{\sqrt{C_k^m C_{k'}^m}} C_k^m \delta_{kk'} = \delta_{kk'}. \end{aligned} \quad (\text{A.4})$$

References

- [1] W. Bao, M.H. Chai, A uniformly convergent numerical method for singularly perturbed nonlinear eigenvalue problems, *Commun. Comput. Phys.* 4 (2008) 135–160.
- [2] W. Bao, I.-L. Chern, F.Y. Lim, Efficient and spectrally accurate numerical methods for computing ground and first excited states in Bose–Einstein condensates, *J. Comput. Phys.* 219 (2006) 836–854.
- [3] W. Bao, Q. Du, Computing the ground state solution of Bose–Einstein condensates by a normalized gradient flow, *SIAM J. Sci. Comput.* 25 (2004) 1674–1697.
- [4] W. Bao, Y. Ge, D. Jaksch, P.A. Markowich, R.M. Weishäupl, Convergence rate of dimension reduction in Bose–Einstein condensates, *Comput. Phys. Commun.* 177 (2007) 832–850.
- [5] W. Bao, F.Y. Lim, Computing ground states of spin-1 Bose–Einstein condensates by the normalized gradient flow, *SIAM J. Sci. Comput.* 30 (2008) 1925–1948.
- [6] W. Bao, J. Shen, A Fourth-order time-splitting Laguerre–Hermite pseudo-spectral method for Bose–Einstein condensates, *SIAM J. Sci. Comput.* 26 (2005) 2010–2028.
- [7] W. Bao, H. Wang, A mass and magnetization conservative and energy diminishing numerical method for computing ground state of spin-1 Bose–Einstein condensates, *SIAM J. Numer. Anal.* 45 (2007) 2177–2200.
- [8] W. Bao, H. Wang, P.A. Markowich, Ground, symmetric and central vortex states in rotating Bose–Einstein condensates, *Commun. Math. Sci.* 3 (2005) 57–88.
- [9] Y. Castin, Z. Hadzibabic, S. Stock, J. Dalibard, S. Stringari, Quantized vortices in the ideal Bose gas: a physical realization of random polynomials, *Phys. Rev. Lett.* 96 (2006). article 040405.
- [10] M.L. Chiofalo, S. Succi, M.P. Tosi, Ground state of trapped interacting Bose–Einstein condensates by an explicit imaginary-time algorithm, *Phys. Rev. E* 62 (2000) 7438–7444.
- [11] B.-Y. Guo, J. Shen, Laguerre–Galerkin method for nonlinear partial differential equations on a semi-infinite interval, *Numer. Math.* 86 (2000) 635–654.
- [12] B.-Y. Guo, J. Shen, C.-L. Xu, Spectral and pseudospectral approximations using Hermite functions: application to the Dirac equation, *Adv. Comput. Math.* 19 (2003) 35–55.
- [13] B.-Y. Guo, X.-Y. Zhang, A new generalized Laguerre spectral approximation and its applications, *J. Comput. Appl. Math.* 181 (2005) 342–363.
- [14] C. Huepe, L.S. Tuckerman, S. Metens, M.E. Brachet, Stability and decay rates of nonisotropic attractive Bose–Einstein condensates, *Phys. Rev. A* 68 (2003). article 023609.
- [15] K.T. Kapale, J.P. Dowling, Vortex phase qubit: Generating arbitrary, counterrotating, coherent superpositions in Bose–Einstein condensates via optical angular momentum beams, *Phys. Rev. Lett.* 95 (2005) 173601.
- [16] I.K. Khabibrakhmanov, D. Summers, The use of generalized Laguerre polynomials in spectral methods for nonlinear differential equations, *Comput. Math. Appl.* 36 (1998) 65–70.
- [17] A. Klein, D. Jaksch, Y. Zhang, W. Bao, Dynamics of vortices in weakly interacting Bose–Einstein condensates, *Phys. Rev. A* 76 (2007). article 043602.
- [18] A.E. Leanhardt, A. Gorlitz, A.P. Chikkatur, D. Kielpinski, Y. Shin, D.E. Pritchard, W. Ketterle, Imprinting vortices in a Bose–Einstein condensate using topological phases, *Phys. Rev. Lett.* 89 (2002). article 190403.
- [19] E.H. Lieb, R. Seiringer, J. Yngvason, Bosons in a trap: a rigorous derivation of the Gross–Pitaevskii energy functional, *Phys. Rev. A* 61 (2000) 3602.
- [20] H. Ma, W. Sun, T. Tang, Hermite spectral methods with a time-dependent scaling for parabolic equations in unbounded domains, *SIAM J. Numer. Anal.* 43 (2005) 58–75.
- [21] K.W. Madison, F. Chevy, W. Wohlgemuth, J. Dalibard, Vortex formation in a stirred Bose–Einstein condensate, *Phys. Rev. Lett.* 84 (2000) 806–809.
- [22] M.R. Matthews, B.P. Anderson, P.C. Haljan, D.S. Hall, C.E. Wieman, E.A. Cornell, Vortices in a Bose–Einstein condensate, *Phys. Rev. Lett.* 93 (1999) 2498.
- [23] P. Muruganandam, S.K. Adhikari, Bose–Einstein condensation dynamics in three dimensions by the pseudospectral and finite-difference methods, *J. Phys. B-At. Mol. Opt. Phys.* 36 (2003) 2501–2513.
- [24] L.P. Pitaevskii, S. Stringari, *Bose–Einstein Condensation*, Clarendon Press, 2003.
- [25] D.S. Rokhsar, Vortex stability and persistent currents in trapped Bose-gas, *Phys. Rev. Lett.* 79 (1997) 2164–2167.
- [26] J. Shen, Stable and efficient spectral methods in unbounded domains using Laguerre functions, *SIAM J. Numer. Anal.* 38 (2000) 1113–1133.
- [27] G. Szegő, *Orthogonal Polynomials*, fourth ed., Amer. Math. Soc. Colloq. Publ. 23, AMS, Providence, RI, 1975.
- [28] T. Tang, The Hermite spectral method for Gaussian-type functions, *SIAM J. Sci. Comput.* 14 (1993) 594–606.
- [29] J.-M. Wu, L.-J. Shen, Spectral analysis of the first-order Hermite cubic spline collocation differentiation matrices, *J. Comput. Math.* 20 (2002) 551–560.
- [30] C.-L. Xu, B.-Y. Guo, Laguerre pseudospectral method for nonlinear partial differential equations, *J. Comput. Math.* 20 (2002) 413–428.
- [31] Y. Zhang, W. Bao, H. Li, Dynamics of rotating two-component Bose–Einstein condensates and its efficient computation, *Phys. D: Nonlinear Phenom.* 234 (2007) 49–69.